JCB

Report

# Sphingolipids activate the endoplasmic reticulum stress surveillance pathway

Francisco Piña,[1]* Fumi Yagisawa,[1]* Keisuke Obara,[2] J.D. Gregerson,[1] Akio Kihara,[2] and Maho Niwa[1]

[1]Division of Biological Sciences, Section of Molecular Biology, University of California, San Diego, La Jolla, CA
[2]Faculty of Pharmaceutical Sciences, Hokkaido University, Sapporo, Japan

Proper inheritance of functional organelles is vital to cell survival. In the budding yeast, *Saccharomyces cerevisiae*, the endoplasmic reticulum (ER) stress surveillance (ERSU) pathway ensures that daughter cells inherit a functional ER. Here, we show that the ERSU pathway is activated by phytosphingosine (PHS), an early biosynthetic sphingolipid. Multiple lines of evidence support this: (1) Reducing PHS levels with myriocin diminishes the ability of cells to induce ERSU phenotypes. (2) Aureobasidin A treatment, which blocks conversion of early intermediates to downstream complex sphingolipids, induces ERSU. (3) *orm1Δorm2Δ* cells, which up-regulate PHS, show an ERSU response even in the absence of ER stress. (4) Lipid analyses confirm that PHS levels are indeed elevated in ER-stressed cells. (5) Lastly, the addition of exogenous PHS is sufficient to induce all ERSU phenotypes. We propose that ER stress elevates PHS, which in turn activates the ERSU pathway to ensure future daughter-cell viability.

## Introduction

The ER is an essential organelle that serves as the birthplace for secretory and membrane proteins and ensures their correct folding and assembly. Moreover, it is a major site for lipid synthesis. When functional demands on the ER exceed its capacity, unfolded and misfolded proteins accumulate in the ER lumen, resulting in a condition known as ER stress. The importance of maintaining ER homeostasis is reflected in the fact that ER stress contributes to human diseases, including type 2 diabetes (Crunkhorn, 2015; Han and Kaufman, 2016), Alzheimer's disease, and Parkinson's disease (Tabas and Ron, 2011; Mercado et al., 2013; Plácido et al., 2014). Molecularly, ER stress induces a well-characterized cellular defense pathway known as the unfolded protein response (UPR), which acts to up-regulate the transcription of genes encoding ER-resident chaperones and protein-modifying enzymes needed to restore ER homeostasis (Mori, 2000; Rutkowski and Kaufman, 2004; Denic et al., 2006; Ron and Walter, 2007; Feige and Hendershot, 2011; Frakes and Dillin, 2017).

Because the ER is not synthesized de novo, but arises from the preexisting ER, transmission of a fully functional ER to the daughter cell is critical during cell division. Under conditions in which the demands on ER function are increased, termed "ER stress," the ER stress surveillance (ERSU) pathway is activated to prevent transmission of a potentially damaged ER into the forming daughter cell in yeast, *Saccharomyces cerevisiae*. The ER that surrounds the nucleus is termed "perinuclear ER" (pnER) in yeast, and the ER localized under the cell cortex is termed the "cortical ER" (cER; Prinz et al., 2000; Du et al., 2001; Fehrenbacher et al., 2002; Estrada et al., 2003; West et al., 2011). pnER and cER are connected by a few ER tubules. The first recognizable step during ER inheritance is entry of the tubular ER emerging from the pnER into the daughter cell. On anchoring of the tubular ER at the bud tip, the ER spreads laterally throughout the daughter cell cortex to generate the cER. In contrast, under ER stress, the pnER and the nucleus enter into the daughter cell, whereas cER inheritance is blocked. Ultimately, ERSU pathway activation delays cytokinesis, in part by causing septin ring mislocalization until ER function is restored (Fig. 1 a; Babour et al., 2010; Piña and Niwa, 2015; Piña et al., 2016). The ERSU pathway ensures that daughter cells inherit functional ER.

Surprisingly, we found that the ERSU pathway is independent of the well-studied UPR, which is also initiated by ER stress. Rather, we showed the ERSU pathway involves activation of a MAP kinase, Slt2, and its upstream kinases, including Pkc1. Cells lacking Slt2 are unable to halt the cell cycle under conditions of ER stress, and the daughter cell therefore inherits a damaged ER, and ultimately, both mother and daughter die. Thus, the ERSU pathway plays a fundamentally critical role in the survival of ER-stressed cells. Currently, we do not know what components are the targets for activated Slt2 kinase under ER stress or what other molecules might be involved in initiating the ERSU.

*F. Piña and F. Yagisawa contributed equally to this paper.

Correspondence to Maho Niwa: niwa@ucsd.edu

F. Yagisawa's present address is Center for Research Advancement and Collaboration, University of the Ryukyu, Nishihara, Japan.



The Rockefeller University Press
J. Cell Biol. Vol. 217 No. 2 495–505
https://doi.org/10.1083/jcb.201708068

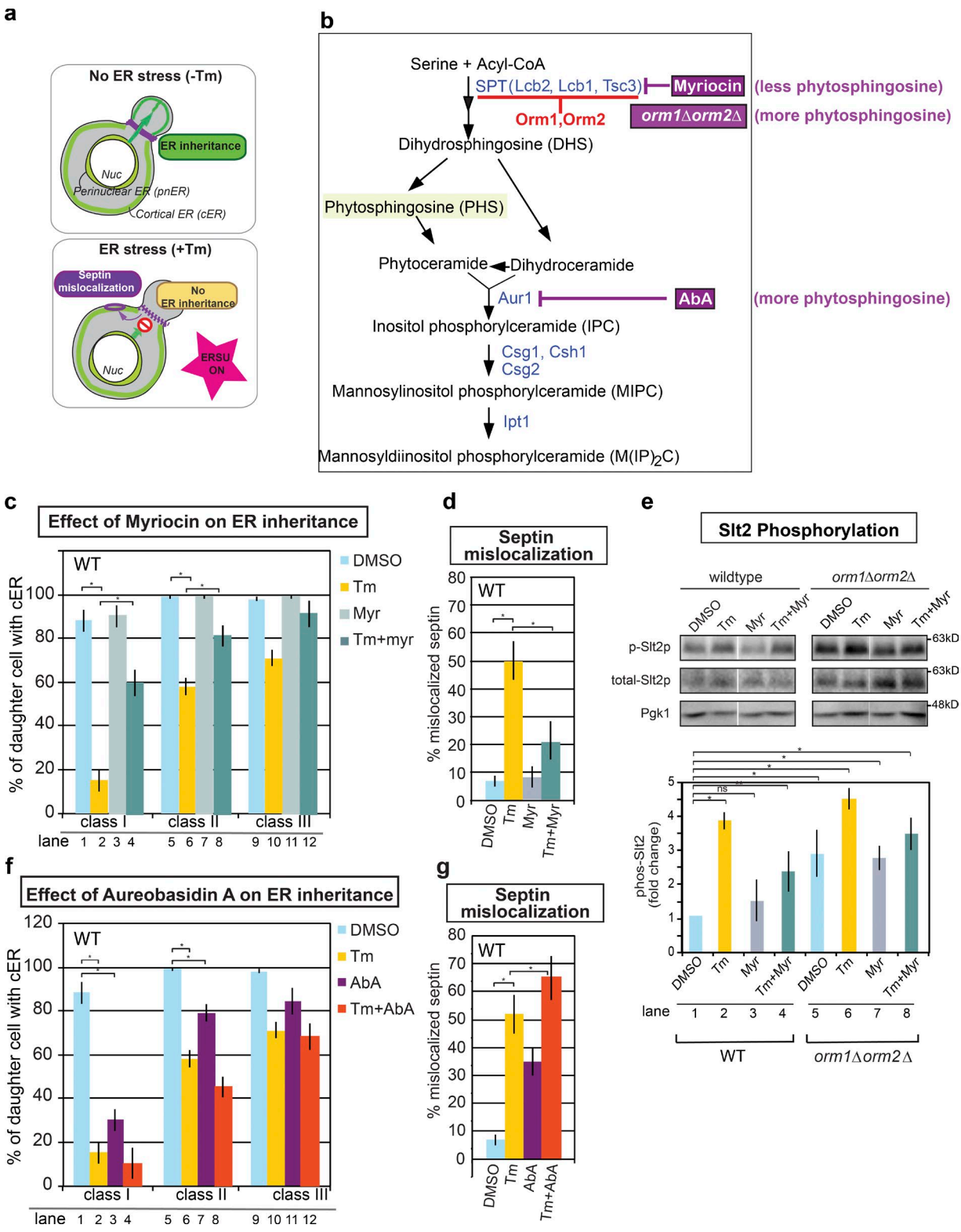


Figure 1. **Inhibitors of the sphingolipid biosynthetic pathway affect ERSU activation. (a)** ER stress activates the ERSU pathway, which blocks cER inheritance and causes septin-ring mislocalization, leading to a cytokinesis arrest. **(b)** A simplified diagram of early steps in the sphingolipid biosynthetic pathway in yeast. A portion only relevant to this study is shown. Some genes were omitted for simplicity; biosynthetic components are in blue, inhibitory genes in red, and inhibitors in purple boxes. The effect of inhibitors to PHS levels are indicated. **(c and d)** WT cells were incubated with or without Tm, a glycosylation inhibitor. All the drug concentrations used throughout this study were described in Materials and methods, unless otherwise stated. The effect of myriocin was tested by preincubating cells with myriocin (Myr) before induction of ER stress by Tm in SC containing 1 M sorbitol. Light blue (DMSO), yellow (+Tm), gray (+Myr), and dark green (Tm + Mry) bars represent the percentage of cells with cER (visualized by Hmg1-GFP reporter) in the daughter cell (c). Sorbitol was added to prevent effects of the cell wall response pathway in all experiments, unless otherwise stated. Cells were classified according to bud size: class I (bud < 2 µm); class II (bud > 2 µm), which lack pnER; and class III, which contain pnER. Quantification of WT cells with mislocalized septin

A recent study revealed that ER stress also expands the overall amount of the ER membrane independently of the UPR (Schuck et al., 2009). It therefore seemed possible that molecules involved in initiating the ERSU pathway might also play a role in coordinating ER size with the cell cycle. It is well known that the majority of yeast lipids, including phospholipids, sphingolipids, and sterols, are synthesized on the exterior face of the ER. However, a few studies focusing on UPR have identified sphingolipids as ER homeostasis regulators (Breslow et al., 2010; Han et al., 2010). Here, we investigated the role of sphingolipid biosynthesis in activating the ERSU pathway and its control of cER inheritance.

## Results and discussion

### ERSU pathway induction is sensitive to sphingolipid alteration

To investigate a potential involvement of sphingolipids in the ERSU pathway (Fig. 1 a), we used a potent sphingolipid biosynthetic pathway inhibitor, myriocin. It inhibits serine palmitoyltransferase (SPT), which converts serine and palmitoyl CoA into 3-ketosphinganine, which is then converted to dihydrosphingosine (Fig. 1 b; Miyake et al., 1995). Myriocin treatment reduces sphingolipid levels in mammalian cells (Miyake et al., 1995; Meyer et al., 2012; Caretti et al., 2016; Salaun et al., 2016). Importantly, this drug is similarly effective in *S. cerevisiae* (Sun et al., 2000; Breslow et al., 2010; Huang et al., 2012; Vecer et al., 2014). Here we used WT cells to examine the effects of myriocin on the ERSU pathway hallmark events: (1) cER inheritance block, (2) septin ring mislocalization, and (3) Slt2 phosphorylation. As a control, we treated cells with tunicamycin (Tm) alone, an *N*-glycosylation inhibitor known to induce ER stress and to block ER inheritance. The typical assay to quantify ER inheritance block involves dividing cells into three classes, based on bud size and inheritance of cortical and pnER, as previously described (Babour et al., 2010; Piña and Niwa, 2015; Piña et al., 2016). Class I cells are those in the early stages of the cell cycle with a small bud (<2 µm in diameter). Class II cells have a medium-size bud (≥2 µm) that lacks pnER. Class III cells have a large bud that contains pnER (Fig. 1 c and Fig. S1 a). In agreement with our previous study, ER stress (i.e., Tm treatment) reduced the number of daughter cells that inherited cER in all three classes of cells (Fig. 1 c, compare yellow and blue bars). This block was specific to cER transmission, in agreement with our previous observations. Myriocin pretreatment for 30 min, however, reduced the ER stress-induced (Tm) cER inheritance block (Fig. 1 c, dark green vs. yellow bars; and Fig. S1 a). Myriocin alone did not block cER inheritance (Fig. 1 c, gray bars; and Fig. S1 a). The impact of ER stress is most significant for class I cells. Many of class II and III cells represent cells that had already inherited the cER in the bud before ER stress induction. We showed previously that cells with cER in the daughter cells at the time of addition of the ER stress inducer do not lose their cER (Piña and Niwa, 2015). Our data has revealed that such cells undergo cytokinesis for the first round but block the cER inheritance during the second round of cell cycle.

Another key ERSU event is septin ring mislocalization away from the bud neck in response to ER stress (Babour et al., 2010). The septin ring normally forms at the site of septation between the two cells before cytokinesis. Thus, septin mislocalization helps establish the ERSU cell cycle block. We followed the septin ring with Shs1-GFP (Babour et al., 2010; Piña and Niwa, 2015; Piña et al., 2016), and as reported, Tm-induced ER stress increased the percentage of cells with mislocalized septin rings (Fig. 1 d, yellow bar; Babour et al., 2010; Piña and Niwa, 2015; Piña et al., 2016). The prevalence of septin ring mislocalization was reduced when cells were pretreated with myriocin before ER stress induction (Fig. 1 d, compare dark green and yellow bars; and Fig. S1 b).

An additional key ERSU event is the activation (phosphorylation) of Slt2, a key ERSU pathway regulator under ER stress (Fig. 1 e; Babour et al., 2010; Piña and Niwa, 2015; Piña et al., 2016). Treating ER-stressed cells with myriocin (i.e., Tm plus myriocin) was found to reduce the levels of Slt2 phosphorylation (Fig. 1 e, p-Slt2p, lane 2 vs. 4).Collectively, the results in Fig. 1 (b–e) reveal that the inhibition of sphingolipid synthesis by myriocin diminishes the ability of Tm-induced ER stress to activate the ERSU pathway: lowered cER inheritance block, decreased septin ring mislocalization, and decreased Slt2 activation.

To further investigate the potential impact of sphingolipid biosynthesis on the ERSU pathway, we performed similar experiments treating cells with the Aur1 inhibitor, aureobasidin A (AbA), which prevents the conversion of phytoceramide or dihydroceramide (DHC) to inositol-phosphoceramide (IPC) and downstream complex sphingolipids, thereby causing the accumulation of upstream PHS (Fig. 1 b; Heidler and Radding, 1995). Like myriocin, AbA is a well-established inhibitor (Nagiec et al., 1997; Zhong et al., 1999; Aeed et al., 2009; Muir et al., 2014). Treating cells with both AbA and Tm lowered cER inheritance, increased septin ring mislocalization, and caused Slt2 phosphorylation compared with Tm treatment alone (Fig. 1, f and g, red; and Fig. 2 h, Tm+AbA, lane 4). Importantly, AbA alone was sufficient to induce the cER inheritance block, septin-ring mislocalization, and Slt2 phosphorylation (Fig. 1, f and g, purple; and Fig. 2 h, AbA, lane 3). The negative impact of myriocin on the ERSU pathway (myriocin reduced levels of ER inheritance block and septin mislocalization when compared with Tm; Fig. 1, c–e) and the positive impact of AbA on the ERSU pathway (AbA increased levels of ER inheritance block and septin mislocalization; Fig. 1, f and g; and Fig. 2 h) suggest that sphingolipid biosynthetic genes or products upstream of Aur1 activate the ERSU pathway. Furthermore, these genes or products must be

was visualized by Shs1-GFP (d). **(e)** Slt2 phosphorylation (p-Slt2p) in WT and *orm1Δorm2Δ* cells, activated with Tm, was attenuated by Myr treatment. Western blots showing levels of phosphor-Slt2 for WT and *orm1Δorm2Δ* cells. The same blot was reprobed with anti-total Slt2 and Pgk1 antibodies. Levels of phosphor-Slt2 in different treatments were normalized based on Pgk1 levels. Fold changes of phosphor-Slt2 levels for both WT and *orm1Δorm2Δ* cells were calculated based on the level of p-Slt2 in DMSO-treated WT cells. The total level of Slt2 protein changed in response to ER stress because of the Hac1 independent transcriptional increase of SLT2 induced by ER stress (Chen et al., 2005; (Babour et al., 2010). **(f and g)** Cells were incubated with (yellow) or without (light blue) Tm in the presence (purple) or absence (red) of 50 ng/ml AbA for 3 h in SC with 1 M sorbitol to assess cER inheritance block (f) or for 2 h to assess mislocalized septin (g). For all quantitation shown in this figure: *, $P < 0.01$; **, $P < 0.05$. Data are the mean ± SD of three independent experiments; $n > 100$ cells of each strain.

associated with processes between the SPT and Aur1 steps of the sphingolipid synthesis pathway (Fig. 1 b).

### Genetic up-regulation of phytosphingosine (PHS) induces ERSU

To further test the role of sphingolipids in activating the ERSU pathway, we examined the involvement of Orm1 and Orm2, evolutionarily conserved negative regulators of SPT activity, which help maintain lipid homeostasis (Fig. 1 b; Breslow et al., 2010; Walther, 2010; Liu et al., 2012). Orm2 functions in the ER stress response, but the exact roles it plays in this response remains elusive (Breslow et al., 2010; Han et al., 2010; Liu et al., 2012). Cells lacking Orm1 and Orm2 (*orm1Δorm2Δ*) showed increased levels of sphingolipids (discussed later in Fig. 5 c). A significant number exhibited cER inheritance block, even before ER stress induction (Fig. 2, a and b, compare WT with *orm1Δorm2Δ*, blue bars, lane 1 vs. 7, 9 vs. 15, and 17 vs. 23; and Fig. S2, a and b). ER stress further increased the number of *orm1Δorm2Δ* cells without cER in their daughter cells (Fig. 2, a and b, compare WT with *orm1Δorm2Δ*, yellow bars, lane 2 vs. 8, 10 vs. 16, and 18 vs. 24; and Fig. S2, a and b). The number of cells with septin ring mislocalization was elevated in *orm1Δorm2Δ* cells before ER stress (Fig. 2 c, compare WT to *orm1Δorm2Δ*, blue bars, lane 1 vs. 7; and Fig. S2 c). ER stress led to more septin-ring mislocalization (Fig. 2 c, lane 7 vs. 8; and Fig. S2 c). Slt2 Phosphorylation followed a similar trend: it was elevated in *orm1Δorm2Δ* cells compared with WT (p-Slt2p; Fig. 2 h, lane 1 vs. 5) and was further increased by Tm-induced ER stress (Fig. 2 h, lane 5 vs. 6). Collectively, the lack of Orm1 and Orm2, which increases sphingolipid biosynthesis, induced all three ERSU phenotypes, even in the unperturbed state, and ER stress exacerbated these ERSU phenotypes (ER inheritance block, septin mislocalization, and Slt2 phosphorylation), supporting the idea that increased levels of sphingolipids activate the ERSU pathway.

The effects of sphingolipid biosynthesis on the ERSU pathway were further examined by adding either myriocin or AbA to *orm1Δorm2Δ* cells. Treatment of *orm1Δorm2Δ* cells with myriocin diminished the levels of ER inheritance block and septin-ring mislocalization, compared with Tm alone (Fig. 2, d and e, compare blue, yellow, and dark green; and Fig. S2, d and e). Addition of AbA alone caused an ER inheritance block and septin mislocalization at levels similar to Tm (Fig. 2, f and g, compare purple with yellow bars; and Fig. S2, d and e). AbA plus ER stress further exacerbated these phenotypes (Fig. 2, f and g, red bars; and Fig. S2, d and e). Thus, these results further support the hypothesis that elevated levels of sphingolipid biosynthesis activate the ERSU pathway.

### Exogenous PHS addition induces ERSU pathway

We reasoned that if an increase in early sphingolipid levels activates the ERSU pathway, then exogenous addition of sphingolipid intermediates might be sufficient to induce ERSU-mediated events. Indeed, WT cells treated with 20 µM PHS increased the number of cells lacking cER in the daughter cells (Fig. 3, a–c, dark brown bars in panel c). Both cER inheritance block and septin ring mislocalization occurred effectively even at 1 µM PHS (Fig. 3, c and e, WT, and red bars in panel c). Interestingly, we noted that when treated with PHS, many class II daughter cells had only tubular ER in daughter cells instead of the fully extended cER (Fig. 3, a and b, WT). We termed these cells to have "partially" inherited ER. Previous studies reported that initial ER inheritance under normal WT conditions (no ER stress) consists of at least three distinct steps: (1) entry of tubular ER extending off the mother nuclear ER into the daughter cell, (2) anchoring of this tubular ER at the bud tip, and (3) expansion of the cER throughout the cortex of the daughter cell (Fehrenbacher et al., 2002). Notably, anchoring of the tubular ER at the bud tip appears to be a critical step for the retention of cER in the daughter cell; before the anchoring step, tubular ER remains uncommitted and could return to the mother cell (West et al., 2011; Chao et al., 2014). We concluded that exogenous PHS addition to unstressed cells does not seem to allow the tubular ER to anchor properly or the cER to spread in the daughter cell (Fig. 3 b). Moreover, we noted that even a longer incubation with PHS never produced cER spread throughout the cortex of the daughter cell.

In addition to the ER inheritance block, addition of PHS also caused septin ring mislocalization (Fig. 3, d and e, WT, lanes 3–5). In addition, we found that the PHS-mediated ER inheritance block and septin mislocalization depends on the presence of Slt2, the MAPK activated in an ERSU pathway; PHS did not have a significant effect on *slt2Δ* cells (Fig. 3, b–e, *slt2Δ*). Finally, we found that addition of PHS also induced Slt2 phosphorylation and that this depends on Pkc1 (Fig. 3 f). The Pkc1 kinase is a component of the ERSU pathway known to function upstream of Slt2. Notably, Slt2 phosphorylation shows a sustained increase during the 120 min of Tm treatment (Fig. 3 f, lanes 1–3) but was observed here to be transient in PHS-treated cells (Fig. 3 f, lanes 4–6), most likely because of PHS conversion to downstream lipid (discussed further in the next section). Importantly, we found that DHC or ceramide could not activate the ERSU pathway, revealing that PHS specifically activates the ERSU pathway (Fig. 4, a–d).

### Sphingolipid analysis confirms PHS increases during the ERSU response

The effects of myriocin, AbA, and *orm1Δorm2Δ* on ERSU phenotypes and the induction of the ERSU phenotypes on addition of PHS are all consistent with the idea that the ERSU pathway is activated by increased levels of PHS. These observations suggest that ER stress causes changes in sphingolipid levels, which could act as an ERSU activating signal. To test if sphingolipid levels are altered in response to ER stress, we measured the levels of components along the sphingolipid pathway (Fig. 1 b), including ceramide, IPC, mannose-inositol-phosphoceramide (MIPC), or $M(IP)_2C$ after ER stress induction (Fig. 5 a and Fig. S3, c and d). First, cells were pulse-labeled with [$^{14}$C]serine, followed by lipid extraction and analysis on TLC to examine the levels of newly synthesized ceramide, IPC, and MIPC in ER-stressed WT cells (Fig. 5 a). Analysis revealed that they increased over the first 30 min followed by a mild decline (Fig. 5 a). Levels of $M(IP)_2C$, the final biosynthetic product of this pathway, continued to increase over the time course of the experiment (Fig. 5 a). Similar increases and subsequent declines in these lipids were observed in Tm-treated *wsc1Δ* cells (Fig. 5 b), consistent with the idea that ER stress-induction of sphingolipids does not require Wsc1 and acts upstream of Wsc1. Wsc1 is a component of the ERSU pathway and thought to function upstream of Slt2. Indeed, both Wsc1 and Slt2 knockout cells were found to display similar ERSU-deficient phenotypes (Fig. 2, b and c), in agreement with our previous study (Babour et al., 2010).

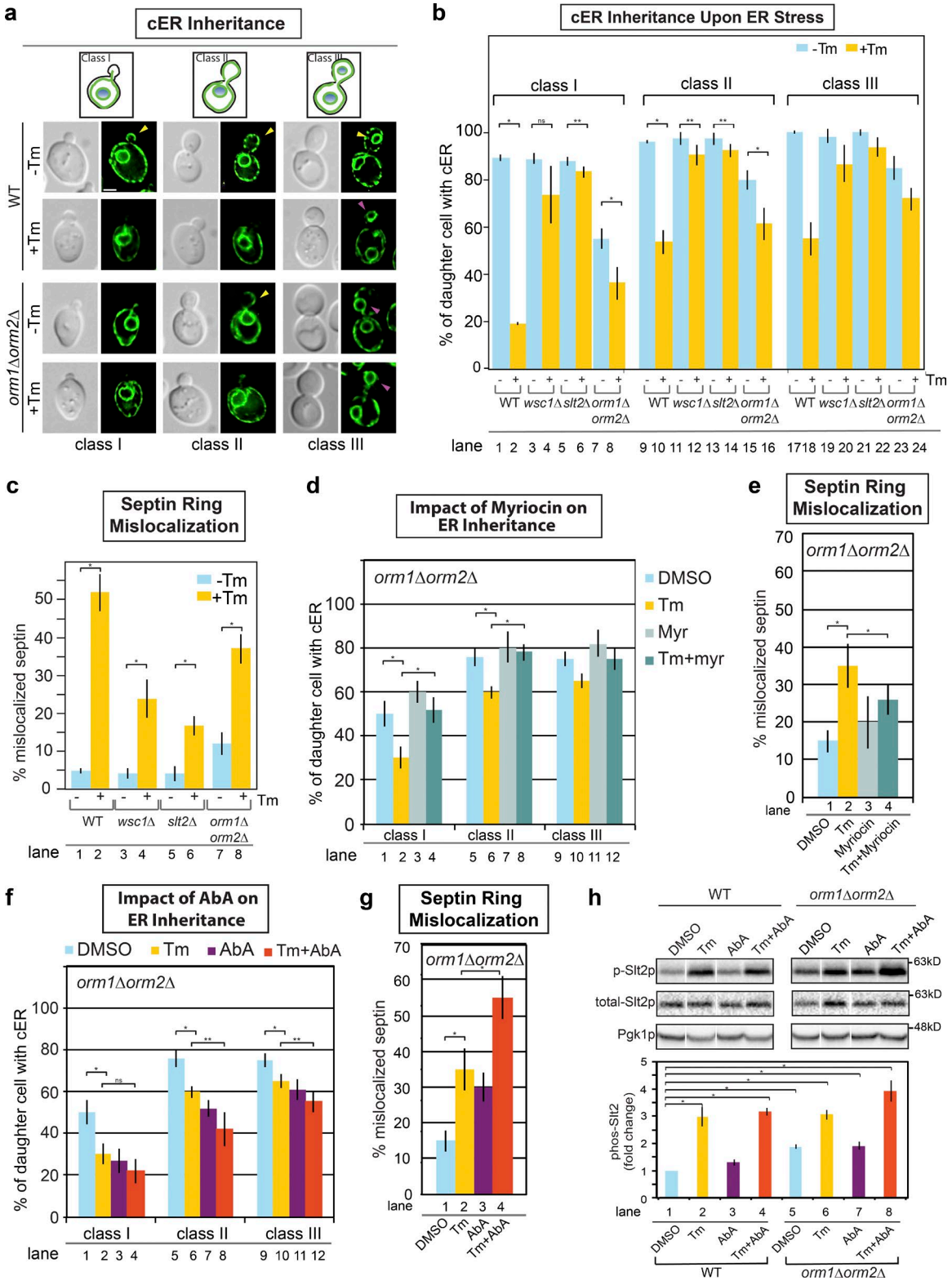


Figure 2. **ERSU activation is altered in *orm1Δorm2Δ* cells. (a)** Differential interference contrast (DIC) and fluorescence microscopy of Hmg1-GFP–expressing WT and *orm1Δorm2Δ* cells. Bar, 2 µm. Yellow arrowheads indicate cER, and magenta arrowheads indicate pnER in the daughter cell. **(b)** Quantification of cER inheritance and mislocalized septin ring in WT, *wsc1Δ*, *slt2Δ*, and *orm1Δorm2Δ* daughter cells. *wsc1Δ* and *slt2Δ* cells are ERSU-deficient control cells, little cER inheritance block, and little septin ring mislocalization, as described (Babour et al., 2010; Piña and Niwa, 2015; Piña et al., 2016). Cells were incubated with or without 1 µg/ml Tm in YPD for 3 h (b) and 2 h (c). The septin ring is visualized with Shs1-GFP. **(d and e)** Cells were incubated with or without Tm after pretreatment with or without Myr for 30 min. Quantification of class I, II, and III *orm1Δorm2Δ* daughter cells containing cER (d) and mislocalized septin (e). **(f and g)** Cells were incubated with or without Tm in the presence or absence of AbA. **(h)** Slt2 phosphorylation in response to Tm and AbA treatment for both WT and *orm1Δorm2Δ* cells. Fold changes of phosphor-Slt2 levels for both WT and *orm1Δorm2Δ* cells were calculated as described in Fig. 1. For all the quantitation shown in this figure, the data are the mean ± SD of three independent experiments; *, $P < 0.01$; **, $P < 0.05$; $n > 100$ cells of each strain.

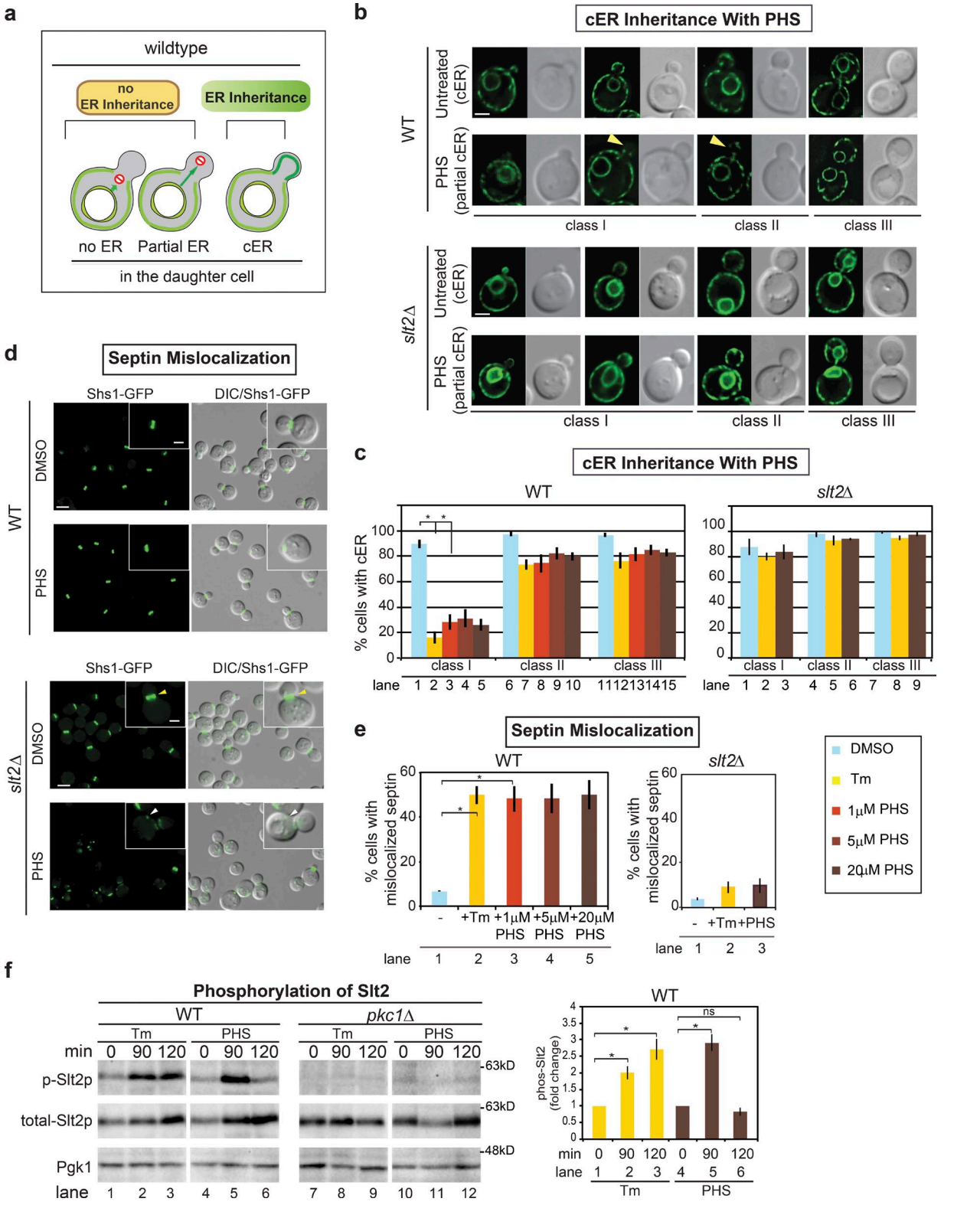


Figure 3. **Addition of PHS induces the ERSU pathway in an Slt2-dependent manner. (a)** Schematic representation of cells with no, partial, or complete cER inheritance by the daughter cell. **(b)** Representative DIC and GFP images of WT and *slt2Δ* cells with the Hmg-GFP reporter with no, partial, or complete cER in untreated and PHS-treated cells. **(c)** Quantification of cER inheritance in WT cells treated with DMSO; 1, 5, and 20 µM PHS; or 1 µg/ml Tm for 90 min or *slt2Δ* cells treated with DMSO, 20 µM PHS, or 1 µg/ml Tm for 90 min. **(d)** Representative fluorescence and DIC images of septin localization (Shs1-GFP) in WT and *slt2Δ* cells treated with DMSO or 20 µM PHS. Inset in each panel shows a close-up view of the septin ring in one of the cells. **(e)** Quantification of septin mislocalizationin in WT cells treated with DMSO; 1, 5, and 20 µM PHS; or 1 µg/ml Tm for 90 min or *slt2Δ* cells treated with DMSO, 20 µM PHS, or 1 µg/ml Tm for 90 min. **(f)** Slt2 phosphorylation in WT and *pkc1Δ* cells treated with 1 µg/ml Tm or 20 µM PHS for indicated times. Levels of p-Slt2 were quantitated based on total Slt2 and Pgk1 loading controls. All results are the mean ± SD of at least three independent experiments ($n > 100$ cells of each strain and treatment). For statistical analyses: *, $P < 0.01$; **, $P < 0.05$. Bars: (insets) 2 µm; (field of cells) 5 µm.

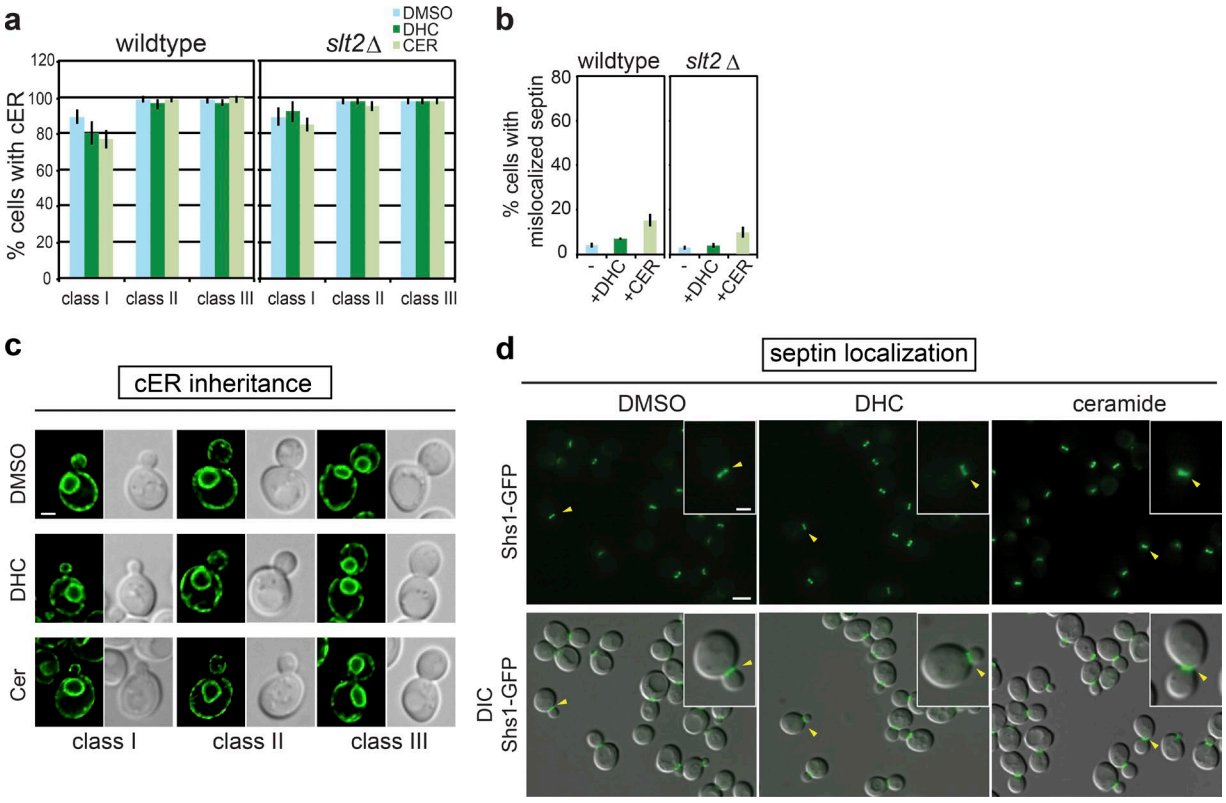


Figure 4. **PHS–induced ERSU is specific. (a and b)** Quantitation of cER inheritance (a) and septin (b) mislocalization in WT and *slt2Δ* cells treated with DMSO, 20 µM DHC, or 20 µM ceramide (Cer). **(c and d)** Representative images of WT cells treated with DMSO, 20 µM DHC, or 20 µM Cer. The insets in the septin panels show a close-up view of the septin ring in one of the cells. Yellow arrowheads indicate normal septin, showing ceramide and DHC have no effect on septin localization. Bars: (insets) 2 µm; (field of cells) 5 µm. All results are the mean ± SD of at least three independent experiments ($n$ > 100 cells of each strain and treatment).

In a separate experiment, ER stress-induced increases were observed for the steady-state levels of PHS in WT cells (Fig. 5 c) examined via mass spectroscopic analysis of unlabeled yeast lipids. Interestingly, the steady-state levels of PHS were significantly elevated up to 20-fold at 90 min in the absence of Orm1 and Orm2 (Fig. 5 c, green line, compare PHS levels in WT and *orm1Δorm2Δ* cells). This is consistent with the inhibitory roles of Orm1 and Orm2 on SPT under normal growth. We noted that a transient increase of PHS did not occur in *orm1Δorm2Δ* cells during ER stress induction (Fig. 5 c), suggesting that Orm1 and Orm2 play roles in the ER stress-induced increase of PHS beyond their inhibitory effects on SPT under normal growth. Importantly, the kinetic increases in the sphingolipid biosynthetic pathway observed here at 30 min preceded the induction of the cER inheritance block and septin mislocalization, which were detectable 30 min after Tm addition and peaked 90 min later (Fig. S3, a and b).

PHS is an early intermediate biosynthetic product that is converted to downstream sphingolipids (Fig. 1 b). Thus, we reasoned that the ERSU phenotypes (ER inheritance block, septin mislocalization, and Slt2 phosphorylation) induced by PHS might be transient because its conversion to downstream sphingolipids takes place in cells. Indeed, the decrease in the levels of phosphorylated Slt2 at 120 min after addition of PHS (Fig. 3 f, lane 6) is consistent with this idea. Thus, we tested the kinetic profiles of the ERSU phenotypes in response to PHS addition and asked if AbA could extend the effect of PHS on the ERSU phenotypes. Specifically, we reasoned that preventing the conversion of phytoceramide to downstream lipids would ultimately build up PHS and thus might extend PHS-induced ERSU events. The number of cells with cER was diminished at 90 min after PHS addition but recovered over 90–180 min of PHS addition (Fig. 5 d). However, in the presence of AbA, the PHS-induced ER inheritance block and septin mislocalization persisted for the full 180 min. These results provide further confirmation that PHS is a key component that induces the ERSU pathway (Fig. 5, d and e; and Fig. S3, g and h). Lastly, we found that the effect of PHS in inducing ERSU is independent of the UPR, because PHS did not activate a UPR enhancer (UPRE)–GFP reporter in WT cells (Fig. 5, f and g).

Our findings indicate that ER stress induces a transient increase in sphingolipids and ceramides. The ER stress-induced increase in PHS, however, is relatively small presumably because it is an early biosynthetic intermediate. Although our results do not rule out the presence of additional ERSU activating components, we found that higher levels of PHS activate ER stress-induced ERSU events including (a) cER inheritance block, (b) septin ring mislocalization, and (c) Slt2 phosphorylation. Key involvement of PHS in the ERSU pathway is supported by several experiments. First, treating cells with myriocin, an inhibitor that decreases PHS levels, lessens the ability of Tm to induce ERSU. Second, treating cells with AbA, an inhibitor that increases PHS levels, induced ER inheritance block and septin ring mislocalization even in the absence of ER stress, and this block is exacerbated by Tm. Third, ERSU events, including Slt2 phosphorylation, are measurable in unstressed *orm1Δorm2Δ*

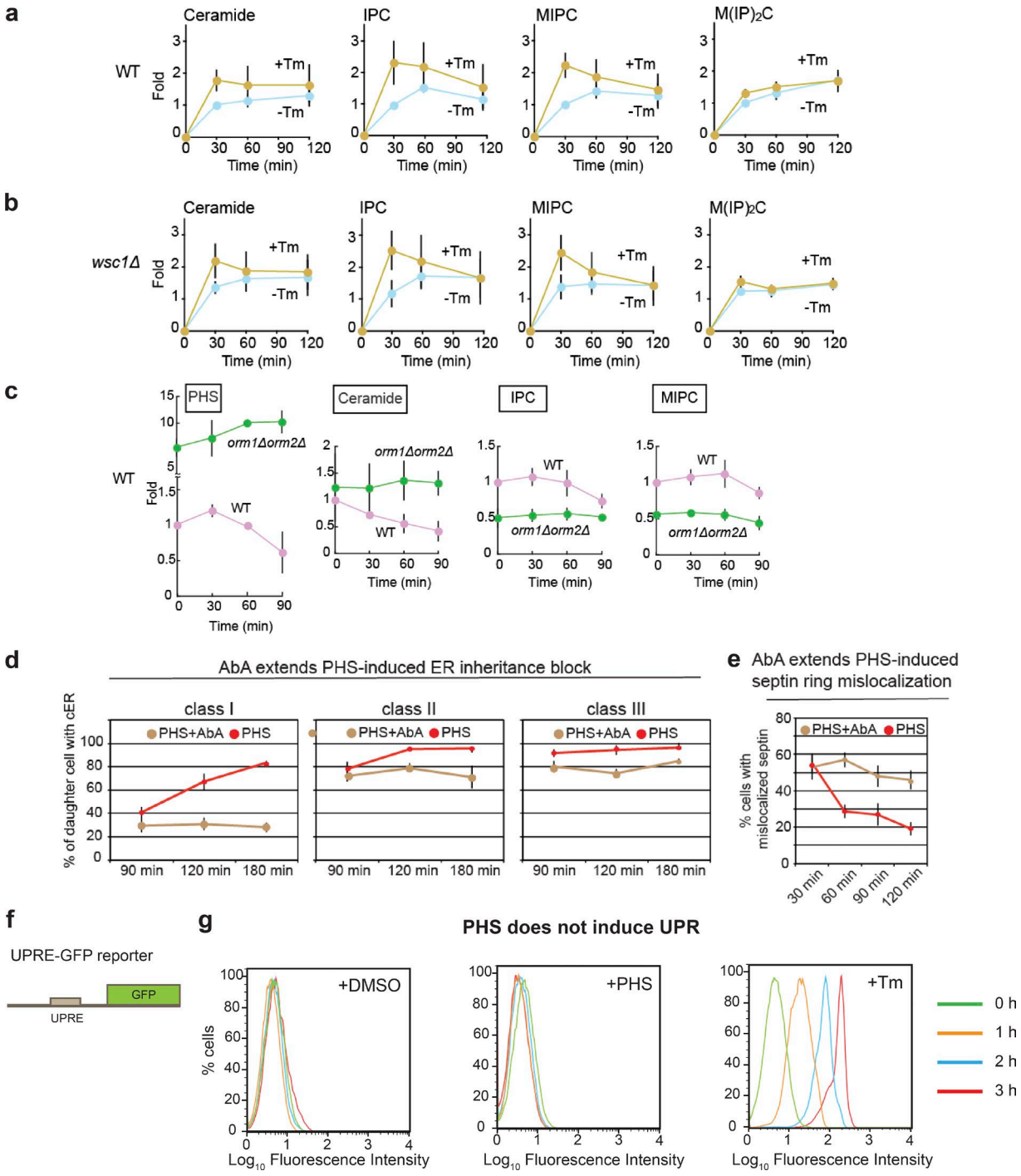


Figure 5. **ER stress induces an increase in sphingolipids.** Production of $^{14}$C-labeled ceramide and complex sphingolipids [IPC, MIPC, and M(IP)$_2$C] in WT and *wsc1Δ* cells after treatment with DMSO or 1 µg/ml Tm for up to 120 min. Lipids were alkali-treated before separation on TLC and quantitated for WT cells (a) and *wsc1*Δ (b). **(c)** Mass spectrometric analysis of sphingolipids (PHS, ceramide, IPC, and MIPC) in WT and *orm1Δorm2Δ* cells treated with 1 µg/ml Tm up to 90 min. Results are the mean ± SD of three independent experiments. **(d and e)** Quantification of cER inheritance (d) and septin-ring mislocalization (e) in WT cells treated with 20 µM PHS (red lines), or 20 µM PHS + 50 ng/ml AbA (brown lines) for the indicated time. **(f)** Schematic showing the UPRE-GFP reporter construct containing the UPRE element fused to the GFP ORF. **(g)** Expression of the UPRE-GFP reporter integrated into the genome of WT cells was measured by flow cytometry. Representative histograms of cell populations treated with DMSO, 1 µg/ml Tm, or 20 µM PHS for the indicated time are shown. All results are the mean ± SD of at least three independent experiments ($n$ > 100 cells of each strain); some error bars are very small and not easy to see.

cells, which contain higher-than-normal PHS levels. Tm treatment of *orm1Δorm2Δ* cells further exacerbates the ER inheritance block and septin mislocalization, although these effects are not as severe as seen in Tm-treated WT cells. Myriocin or AbA had minimal effects on *orm1Δorm2Δ* cells. Fourth, lipid analysis shows that Tm increases phytosphingolipid levels. Perhaps most compellingly, exogenous addition of PHS induces the hallmark responses of the ERSU pathway.

Table 1. **Yeast strains**

| Name | Genotype | Reference |
|---|---|---|
| MNY1428 | *MATa, leu2-3,112, trp1-1, can1-100, ura3-1::HMG1-GFP:URA3, ade2-1, his3-11, bar1Δ::LEU2* | This study |
| MNY1043 | *MATa, leu2-3,112, trp1-1, can1-100, ura3-1::HMG1-GFP:URA3, ade2-1, his3-11,15::UPRE-lacZ:HIS3, slt2Δ::KanMX* | Babour et al., 2010 |
| MNY2076 | *MATa, leu2-3,112, trp1-1, can1-100, ura3-1::HMG1-GFP:URA3, ade2-1, his3-11, bar1Δ::LEU2, wsc1Δ::KanMX* | This study |
| MNY2099 | *MATa, leu2-3,112, trp1-1, SHS1-GFP:TRP1, can1-100, ura3-1, ade2-1, his3-11, bar1::LEU2, wsc1Δ::KanMX* | This study |
| MNY2100 | *MATa, leu2-3,112, trp1-1, SHS1-GFP:TRP1, can1-100, ura3-1, ade2-1, his3-11, bar1Δ::LEU2,* | This study |
| MNY2101 | *MATa, leu2-3,112, trp1-1, SHS1-GFP:TRP1, can1-100, ura3-1, ade2-1, his3-11, bar1Δ::LEU2, slt2Δ::KanMX* | This study |
| MNY2500 | *Mat alpha leu2-3, 112 trp1-1 can1-100 ura3-1::HMG1-GFP:URA3 ade2-1 his3-11, 15* | This study |
| MNY2708 | *Mat alpha leu2-3, 112 trp1-1 can1-100 ura3-1::HMG1-GFP:URA3 ade2-1 his3-11, 15 orm2D::KanMX orm1::NatMX* | This study |
| MNY2712 | *Mat a leu2-3, 112 trp1-1 can1-100 Shs1-GFP::TRP1 ade2-1 his3-11, 15 orm2D::KanMX orm1::NatMX* | This study |
| MNY2434 | *MATa, leu2-3, 112, trp1-1, can1-100, ura3-1::UPRE-GFP::URA3, ade2-1, his3-11,15, bar1Δ::LEU2* | This study |

Collectively, these data indicate that ER stress increased the levels of PHS, which appears to act as a key inducer of the ERSU pathway to block ER inheritance into the daughter cell and halt cytokinesis. This prevents the generation of daughter cells with a functionally compromised ER. Although TLC analyses revealed that IPC, MIPC, and $M(IP)_2C$ were also increased on Tm treatment, these complex sphingolipids are likely not important for ERSU pathway induction for the following reasons: First, treating cells with AbA alone induced the ERSU pathway, suggesting that biosynthetic products upstream of IPC are the critical ones. In addition, exogenous ceramide or DHC, which are just downstream of PHS, were incapable of activating the ERSU pathway, limiting the potential ERSU-relevant bioactive sphingolipids to PHS.

Sphingolipids and their metabolites are known to influence the mammalian cell cycle (Gable et al., 2002; Schuck et al., 2009), but the precise mechanism remains unclear. Sphingolipids activate ERK1/2, a mammalian homologue of the yeast kinase SLT2 (Chang and Karin, 2001). Although it is not clear whether mammalian cells possess an ERSU-like pathway, it is interesting to speculate that changes in sphingolipid levels may also ensure proper inheritance of a functional ER during the mammalian cell cycle. In mammalian cells, asymmetric division and thus, asymmetric apportioning of the ER occurs in certain settings, most notably during the division of stem cells. Therefore, an ERSU-like pathway may play a vital role in ensuring proper segregation of the mammalian ER (and/or other organelles) between the self-renewing stem cell and the differentiating daughter. Thus, PHS induction of the hallmarks of the yeast ERSU pathway lays the foundation to explore mammalian stem cell division.

## Materials and methods

### Strains

The strains used in this study are listed in Table 1. The knockout strains were generated by standard PCR-based methods. Homologous recombination of PCR fragments amplified from the genomic DNA of corresponding yeast knockout collection strains (or the preexisting *orm1Δ* strain; Breslow et al., 2010) was done by using primer pairs (Table 2). The *orm1Δorm2Δ* strain was generated by mating the single knockouts and dissecting the tetrads. The 4×UPRE-GFP strain was prepared by integrating StuI-linearized pRH1209 into the *URA3* locus (Hampton et al., 1996). Cells were grown in yeast extract-peptone-dextrose (YPD) containing 1 M sorbitol or synthetic complete media (SC) containing 1M sorbitol at 30°C, unless otherwise noted. Log-phase cells were used for all analyses.

### Drug treatment

Cells were treated with Tm (Calbiochem) at a final concentration of 1 µg/ml at 30°C for 3 h to analyze cER inheritance and 2 h to analyze septin, unless otherwise noted. Using α-factor–synchronized cells, we have previously shown that cER inheritance and cytokinesis are effectively blocked when Tm is added to small-budded cells before cER inheritance. If cells experience ER stress after cER stably enters into the daughter cell, such cells will divide once, and then cER inheritance and cytokinesis will be blocked in the next round of the cell cycle. A 3-h treatment is sufficient to block ER inheritance in daughter cells, regardless of cell cycle stage (Piña and Niwa, 2015). Myriocin was stored as a stock 200-µM solution in methanol and used at 400 ng/ml. AbA was stored as a stock 2-mg/ml solution in DMSO and used at 50 ng/ml. Myriocin was added to cells 30 min before Tm. AbA was added to the cells at the same time as Tm. PHS (Sigma), C2-DHC (Enzo Life Sciences), and C2-ceramide (Enzo life sciences) were stored as stock 10-mM solutions in DMSO and used at 1, 5, and 20 µM. PHS-, DHC-, and ceramide-treated cells were grown in SC with 1 M sorbitol at 30°C.

### Microscopy

An Axiovert 200M Micro-Imaging microscope (Carl Zeiss) with a 100× 1.3 NA objective was used as described previously (Babour et al., 2010). To quantify ER inheritance, z-stack images with 300-nm intervals were taken, and each plane was examined for presence or absence of cER. Images of cER are z-stack projections after constrained iterative deconvolution.

### Lipid analyses

For the TLC analyses, cells were grown to log phase in serine- and threonine-free SC. For labeling sphingolipids, [$^{14}$C]serine (1 µCi/ml culture; PerkinElmer Life Sciences) was added at the same time as Tm or DMSO. Lipid extraction and TLC analyses were performed as described previously (Kihara et al., 2008). For quantification of ceramide, IPC, and MIPC, lipids were alkali-treated before TLC analysis. $M(IP)_2C$ was analyzed without alkali pretreatment and desalting.

Table 2. **Primers**

| Name | Sequence(5′–3′) | Strain made by using the primers |
|---|---|---|
| OAB200 | GAAGGAACAAGACTTGCTTGGC | *wsc1::KanMX* |
| OAB201 | TTTTCTCCGCCTTTCCTCTCTG | |
| OFY264 | TCAGATGCAGATATTTCAGTGG | *orm1::NatMX* |
| OFY265 | GGTTTAGAAGGTGCATTAATATGG | |
| OFY266 | TCCGCACGTAGAATTAGAGAAT | *orm2::KanMX* |
| OFY267 | TTTGACGTGTACTCCGATGTAA | |

Signals on TLC plates were quantified by using a bioimaging analyzer BAS-2500 (Fuji Photo Film) and then detected by exposure to x-ray film by using a BioMax TranScreen LE intensifying screen (Kodak).

For mass spectrometry, lipids were extracted from yeast cells (5.0 $A_{600}$ units) as described previously (Kihara et al., 2008; Ejsing et al., 2009; Breslow et al., 2010; Kondo et al., 2014) in the presence of d18:1-17:0 ceramide as an internal standard. Lipid extracts were then desalted as follows. The dried lipid film was resuspended in 200 µl water-saturated butanol, and 100 µl water was added and vortexed vigorously. After centrifugation at 9,100 *g* for 2 min, the top butanol phase was recovered. The aqueous phase was reextracted with 200 µl water-saturated butanol. The butanol phases were pooled together and dried. The dried lipid film was resuspended in 100 µl chloroform/methanol/$H_2O$ (5:4:1, vol/vol). Lipids were separated with reversed-phase ultra-performance liquid chromatography as described previously (Kihara et al., 2008; Ejsing et al., 2009; Breslow et al., 2010; Kondo et al., 2014) and analyzed by using electrospray ionization tandem triple quadruple mass spectrometry (Xevo TQ-S; Waters). Ceramide, IPC, and MIPC species with chain-lengths of 18 and 26 for long-chain base and acyl-chain moiety, respectively, were detected by multiple reactions monitored by selecting the *m/z* of specific sphingolipid species at Q1 and the *m/z* 284.2 and *m/z* 282.2 for sphingolipids containing dihydrosphingosine and PHS, respectively, at Q3. The values were normalized with those of the internal standard.

### Flow cytometry

UPR activation levels were analyzed by flow cytometry of cells carrying UPRE-GFP on incubation with Tm, as described previously (Bicknell et al., 2007).

### Slt2 phosphorylation

Extraction and Western blot analyses to examine Slt2 phosphorylation were performed as described previously (Babour et al., 2010). Levels of phosphorylated Slt2 (P-Slt2) were quantitated based on loading control of PGK1 levels.

### Online supplemental material

Fig. S1 shows representative images of cER (Hmg1-GFP) and septin (Shs1-GFP) in ER-stressed or unstressed WT cells treated with myriocin or AbA. Fig. S2 shows representative images of cER and septin in ER-stressed and unstressed *orm1Δorm2Δ* cells. Fig. S3 shows cER and septin in WT cells treated with PHS.

## Acknowledgments

We thank Drs. Peter E. Geiduschek, Douglass Forbes, and David O'Keefe for critical reading of the manuscript and Drs. Lorraine Pillus and Lauren G. Clark for their help in making the *orm1Δorm2Δ* double-knockout cells.

This work was supported by the National Institutes of Health (grant GM087415) and the American Cancer Society (118765-RSG-10-027-01-CSM) to M. Niwa, Allergy postdoctoral training grant (National Institutes of Health 5T32AI007469-20UCSD/LIAI) to F. Piña, and postdoctoral fellowships for research abroad from Japan Society for the Promotion of Science (727) to F. Yagisawa.

The authors declare no competing financial interests.

Author contributions: F. Piña conceptualized; performed the experiments, the investigation, and data analysis; and wrote the paper. F. Yagisawa conceptualized, performed the experiments and data analysis, and wrote the paper. K. Obara performed lipid experiments and analyses. J.D. Gregerson performed the experiments and analysis. A. Kihara conceptualized the lipid analyses and provided advice. M. Niwa conceptualized and provided project administration, data analysis, writing, and funding acquisition.

Submitted: 9 August 2017
Revised: 10 November 2017
Accepted: 29 November 2017

## References

Aeed, P.A., C.L. Young, M.M. Nagiec, and A.P. Elhammer. 2009. Inhibition of inositol phosphorylceramide synthase by the cyclic peptide aureobasidin A. *Antimicrob. Agents Chemother.* 53:496–504. https://doi.org/10.1128/AAC.00633-08

Babour, A., A.A. Bicknell, J. Tourtellotte, and M. Niwa. 2010. A surveillance pathway monitors the fitness of the endoplasmic reticulum to control its inheritance. *Cell.* 142:256–269. https://doi.org/10.1016/j.cell.2010.06.006

Bicknell, A.A., A. Babour, C.M. Federovitch, and M. Niwa. 2007. A novel role in cytokinesis reveals a housekeeping function for the unfolded protein response. *J. Cell Biol.* 177:1017–1027. https://doi.org/10.1083/jcb.200702101

Breslow, D.K., S.R. Collins, B. Bodenmiller, R. Aebersold, K. Simons, A. Shevchenko, C.S. Ejsing, and J.S. Weissman. 2010. Orm family proteins mediate sphingolipid homeostasis. *Nature.* 463:1048–1053. https://doi.org/10.1038/nature08787

Caretti, A., R. Torelli, F. Perdoni, M. Falleni, D. Tosi, A. Zulueta, J. Casas, M. Sanguinetti, R. Ghidoni, E. Borghi, and P. Signorelli. 2016. Inhibition of ceramide de novo synthesis by myriocin produces the double effect of reducing pathological inflammation and exerting antifungal activity against A. fumigatus airways infection. *Biochim. Biophys. Acta.* 1860:1089–1097. https://doi.org/10.1016/j.bbagen.2016.02.014

Chang, L., and M. Karin. 2001. Mammalian MAP kinase signalling cascades. *Nature.* 410:37–40. https://doi.org/10.1038/35065000

Chao, J.T., A.K. Wong, S. Tavassoli, B.P. Young, A. Chruscicki, N.N. Fang, L.J. Howe, T. Mayor, L.J. Foster, and C.J. Loewen. 2014. Polarization of the endoplasmic reticulum by ER-septin tethering. *Cell.* 158:620–632. https://doi.org/10.1016/j.cell.2014.06.033

Chen, Y., D.E. Feldman, C. Deng, J.A. Brown, A.F. De Giacomo, A.F. Gaw, G. Shi, Q.T. Le, J.M. Brown, and A.C. Koong. 2005. Identification of mitogen-activated protein kinase signaling pathways that confer resistance to endoplasmic reticulum stress in Saccharomyces cerevisiae. *Mol. Cancer Res.* 3:669–677. https://doi.org/10.1158/1541-7786.MCR-05-0181

Crunkhorn, S. 2015. Type 2 diabetes: ER stress modulator reverses diabetes. *Nat. Rev. Drug Discov.* 14:528.

Denic, V., E.M. Quan, and J.S. Weissman. 2006. A luminal surveillance complex that selects misfolded glycoproteins for ER-associated degradation. *Cell.* 126:349–359. https://doi.org/10.1016/j.cell.2006.05.045

Du, Y., M. Pypaert, P. Novick, and S. Ferro-Novick. 2001. Aux1p/Swa2p is required for cortical endoplasmic reticulum inheritance in Saccharomyces cerevisiae. *Mol. Biol. Cell.* 12:2614–2628. https://doi.org/10.1091/mbc.12.9.2614

Ejsing, C.S., J.L. Sampaio, V. Surendranath, E. Duchoslav, K. Ekroos, R.W. Klemm, K. Simons, and A. Shevchenko. 2009. Global analysis of the yeast lipidome by quantitative shotgun mass spectrometry. *Proc. Natl. Acad. Sci. USA.* 106:2136–2141. https://doi.org/10.1073/pnas.0811700106

Estrada, P., J. Kim, J. Coleman, L. Walker, B. Dunn, P. Takizawa, P. Novick, and S. Ferro-Novick. 2003. Myo4p and She3p are required for cortical ER inheritance in *Saccharomyces cerevisiae*. *J. Cell Biol.* 163:1255–1266. https://doi.org/10.1083/jcb.200304030

Fehrenbacher, K.L., D. Davis, M. Wu, I. Boldogh, and L.A. Pon. 2002. Endoplasmic reticulum dynamics, inheritance, and cytoskeletal interactions in budding yeast. *Mol. Biol. Cell.* 13:854–865. https://doi.org/10.1091/mbc.01-04-0184

Feige, M.J., and L.M. Hendershot. 2011. Disulfide bonds in ER protein folding and homeostasis. *Curr. Opin. Cell Biol.* 23:167–175. https://doi.org/10.1016/j.ceb.2010.10.012

Frakes, A.E., and A. Dillin. 2017. The UPRER: Sensor and coordinator of organismal homeostasis. *Mol. Cell.* 66:761–771. https://doi.org/10.1016/j.molcel.2017.05.031

Gable, K., G. Han, E. Monaghan, D. Bacikova, M. Natarajan, R. Williams, and T.M. Dunn. 2002. Mutations in the yeast LCB1 and LCB2 genes, including those corresponding to the hereditary sensory neuropathy type I mutations, dominantly inactivate serine palmitoyltransferase. *J. Biol. Chem.* 277:10194–10200. https://doi.org/10.1074/jbc.M107873200

Hampton, R.Y., A. Koning, R. Wright, and J. Rine. 1996. In vivo examination of membrane protein localization and degradation with green fluorescent protein. *Proc. Natl. Acad. Sci. USA*. 93:828–833. https://doi.org/10.1073/pnas.93.2.828

Han, J., and R.J. Kaufman. 2016. The role of ER stress in lipid metabolism and lipotoxicity. *J. Lipid Res.* 57:1329–1338. https://doi.org/10.1194/jlr.R067595

Han, S., M.A. Lone, R. Schneiter, and A. Chang. 2010. Orm1 and Orm2 are conserved endoplasmic reticulum membrane proteins regulating lipid homeostasis and protein quality control. *Proc. Natl. Acad. Sci. USA*. 107:5851–5856. https://doi.org/10.1073/pnas.0911617107

Heidler, S.A., and J.A. Radding. 1995. The AUR1 gene in Saccharomyces cerevisiae encodes dominant resistance to the antifungal agent aureobasidin A (LY295337). *Antimicrob. Agents Chemother.* 39:2765–2769. https://doi.org/10.1128/AAC.39.12.2765

Huang, X., J. Liu, and R.C. Dickson. 2012. Down-regulating sphingolipid synthesis increases yeast lifespan. *PLoS Genet.* 8:e1002493. https://doi.org/10.1371/journal.pgen.1002493

Kihara, A., H. Sakuraba, M. Ikeda, A. Denpoh, and Y. Igarashi. 2008. Membrane topology and essential amino acid residues of Phs1, a 3-hydroxyacyl-CoA dehydratase involved in very long-chain fatty acid elongation. *J. Biol. Chem.* 283:11199–11209. https://doi.org/10.1074/jbc.M708993200

Kondo, N., Y. Ohno, M. Yamagata, T. Obara, N. Seki, T. Kitamura, T. Naganuma, and A. Kihara. 2014. Identification of the phytosphingosine metabolic pathway leading to odd-numbered fatty acids. *Nat. Commun.* 5:5338. https://doi.org/10.1038/ncomms6338

Liu, M., C. Huang, S.R. Polu, R. Schneiter, and A. Chang. 2012. Regulation of sphingolipid synthesis through Orm1 and Orm2 in yeast. *J. Cell Sci.* 125:2428–2435. https://doi.org/10.1242/jcs.100578

Mercado, G., P. Valdés, and C. Hetz. 2013. An ERcentric view of Parkinson's disease. *Trends Mol. Med.* 19:165–175. https://doi.org/10.1016/j.molmed.2012.12.005

Meyer, S.G., A.E. Wendt, M. Scherer, G. Liebisch, U. Kerkweg, G. Schmitz, and H. de Groot. 2012. Myriocin, an inhibitor of serine palmitoyl transferase, impairs the uptake of transferrin and low-density lipoprotein in mammalian cells. *Arch. Biochem. Biophys.* 526:60–68. https://doi.org/10.1016/j.abb.2012.07.006

Miyake, Y., Y. Kozutsumi, S. Nakamura, T. Fujita, and T. Kawasaki. 1995. Serine palmitoyltransferase is the primary target of a sphingosine-like immunosuppressant, ISP-1/myriocin. *Biochem. Biophys. Res. Commun.* 211:396–403. https://doi.org/10.1006/bbrc.1995.1827

Mori, K. 2000. Tripartite management of unfolded proteins in the endoplasmic reticulum. *Cell.* 101:451–454. https://doi.org/10.1016/S0092-8674(00)80855-7

Muir, A., S. Ramachandran, F.M. Roelants, G. Timmons, and J. Thorner. 2014. TORC2-dependent protein kinase Ypk1 phosphorylates ceramide synthase to stimulate synthesis of complex sphingolipids. *Elife.* 3:e03779. https://doi.org/10.7554/eLife.03779

Nagiec, M.M., E.E. Nagiec, J.A. Baltisberger, G.B. Wells, R.L. Lester, and R.C. Dickson. 1997. Sphingolipid synthesis as a target for antifungal drugs. Complementation of the inositol phosphorylceramide synthase defect in a mutant strain of Saccharomyces cerevisiae by the AUR1 gene. *J. Biol. Chem.* 272:9809–9817. https://doi.org/10.1074/jbc.272.15.9809

Piña, F.J., and M. Niwa. 2015. The ER stress surveillance (ERSU) pathway regulates daughter cell ER protein aggregate inheritance. *Elife.* 4:e06970. https://doi.org/10.7554/eLife.06970

Piña, F.J., T. Fleming, K. Pogliano, and M. Niwa. 2016. Reticulons regulate the ER inheritance block during ER stress. *Dev. Cell.* 37:279–288. https://doi.org/10.1016/j.devcel.2016.03.025

Plácido, A.I., C.M. Pereira, A.I. Duarte, E. Candeias, S.C. Correia, R.X. Santos, C. Carvalho, S. Cardoso, C.R. Oliveira, and P.I. Moreira. 2014. The role of endoplasmic reticulum in amyloid precursor protein processing and trafficking: implications for Alzheimer's disease. *Biochim. Biophys. Acta.* 1842:1444–1453. https://doi.org/10.1016/j.bbadis.2014.05.003

Prinz, W.A., L. Grzyb, M. Veenhuis, J.A. Kahana, P.A. Silver, and T.A. Rapoport. 2000. Mutants affecting the structure of the cortical endoplasmic reticulum in *Saccharomyces cerevisiae*. *J. Cell Biol.* 150:461–474. https://doi.org/10.1083/jcb.150.3.461

Ron, D., and P. Walter. 2007. Signal integration in the endoplasmic reticulum unfolded protein response. *Nat. Rev. Mol. Cell Biol.* 8:519–529. https://doi.org/10.1038/nrm2199

Rutkowski, D.T., and R.J. Kaufman. 2004. A trip to the ER: Coping with stress. *Trends Cell Biol.* 14:20–28. https://doi.org/10.1016/j.tcb.2003.11.001

Salaun, E., L. Lefeuvre-Orfila, T. Cavey, B. Martin, B. Turlin, M. Ropert, O. Loreal, and F. Derbré. 2016. Myriocin prevents muscle ceramide accumulation but not muscle fiber atrophy during short-term mechanical unloading. *J. Appl. Physiol. (1985)* 120:178–187. https://doi.org/10.1152/japplphysiol.00720.2015

Schuck, S., W.A. Prinz, K.S. Thorn, C. Voss, and P. Walter. 2009. Membrane expansion alleviates endoplasmic reticulum stress independently of the unfolded protein response. *J. Cell Biol.* 187:525–536. https://doi.org/10.1083/jcb.200907074

Sun, Y., R. Taniguchi, D. Tanoue, T. Yamaji, H. Takematsu, K. Mori, T. Fujita, T. Kawasaki, and Y. Kozutsumi. 2000. Sli2 (Ypk1), a homologue of mammalian protein kinase SGK, is a downstream kinase in the sphingolipid-mediated signaling pathway of yeast. *Mol. Cell. Biol.* 20:4411–4419. https://doi.org/10.1128/MCB.20.12.4411-4419.2000

Tabas, I., and D. Ron. 2011. Integrating the mechanisms of apoptosis induced by endoplasmic reticulum stress. *Nat. Cell Biol.* 13:184–190. https://doi.org/10.1038/ncb0311-184

Vecer, J., P. Vesela, J. Malinsky, and P. Herman. 2014. Sphingolipid levels crucially modulate lateral microdomain organization of plasma membrane in living yeast. *FEBS Lett.* 588:443–449. https://doi.org/10.1016/j.febslet.2013.11.038

Walther, T.C. 2010. Keeping sphingolipid levels nORMal. *Proc. Natl. Acad. Sci. USA*. 107:5701–5702. https://doi.org/10.1073/pnas.1001503107

West, M., N. Zurek, A. Hoenger, and G.K. Voeltz. 2011. A 3D analysis of yeast ER structure reveals how ER domains are organized by membrane curvature. *J. Cell Biol.* 193:333–346. https://doi.org/10.1083/jcb.201011039

Zhong, W., D.J. Murphy, and N.H. Georgopapadakou. 1999. Inhibition of yeast inositol phosphorylceramide synthase by aureobasidin A measured by a fluorometric assay. *FEBS Lett.* 463:241–244. https://doi.org/10.1016/S0014-5793(99)01633-6